

Proton- γ angular correlations in the reaction $^{52}\text{Cr}(d, p\gamma)^{53}\text{Cr}$

W. Eyrich, S. Schneider, A. Hofmann, U. Scheib, and F. Vogler

Physikalisches Institut III der Universität Erlangen-Nürnberg, 8520 Erlangen, Germany

(Received 8 August 1974)

The reaction $^{52}\text{Cr}(d, p\gamma)^{53}\text{Cr}$ has been studied at a deuteron energy of 10 MeV up to an excitation energy in ^{53}Cr of about 5 MeV. The protons have been detected by use of a multidetector arrangement consisting of 8–11 silicon surface-barrier detectors. Particle- γ coincidence measurements have been performed with a Ge(Li) detector in and out of the reaction plane. Absolute double differential cross sections have been measured for particle angles between 20 and 160° for several transitions with l transfers of 1, 2, 3, and 4. From differential and double differential cross sections the experimental particle- γ angular correlation functions as a function of the particle angle have been extracted. The differential cross sections and the angular correlation functions have been analyzed with distorted-wave Born approximation. It turned out that deuteron potentials giving four half wave lengths of the wave function inside the potential well yield the best agreement with both the differential cross sections and the angular correlation functions. The influence of the spin orbit potential on the angular correlation was found to be less important.

NUCLEAR REACTIONS $^{52}\text{Cr}(d, p\gamma)$, $E = 10$ MeV; measured differential and double differential cross sections. DWBA analyses of $l = 1, 3$, and 4 transitions; enriched target.

I. INTRODUCTION

Particle- γ correlation experiments are performed to determine the parameters of the γ transitions, but also to investigate the reaction mechanism. In order to determine the γ transition data it is convenient to measure the correlation functions in dependence on the angles of the γ detector. For that purpose the so-called Ferguson-Litherland II Geometry¹ is often used.

In order to investigate the reaction mechanism the measurement of the correlation function as a function of the particle angle is preferable, because in general the magnitudes of the individual transition amplitudes depend sensitively on the particle angles. In general, particle- γ correlation measurements are more sensitive to the reaction mechanism than measurements of the differential cross section, because in the correlation function mixed phase-dependent terms of transition amplitudes between the magnetic substates are involved. This has been shown² for the inelastic scattering of α particles from ^{26}Mg .

In a previous work³ we studied the reaction $^{24}\text{Mg}(d, p\gamma)^{25}\text{Mg}$ in order to obtain more information about the reaction mechanism. For this reaction it has been found that for some (d, p) transitions neither the differential cross section data nor the correlation data could be described by the distorted-wave Born approximation (DWBA) in a satisfactory way. Thus it seemed advisable to look for a reaction for which DWBA is believed to be an ade-

quate approximation, in order to investigate which additional information can be obtained from angular correlation experiments.

For the reaction $^{52}\text{Cr}(d, p\gamma)^{53}\text{Cr}$ the differential cross sections for several (d, p) transitions with $l = 1, 3$, and 4 are well described by DWBA. Furthermore, the γ data of ^{53}Cr are well known in the studied range of the excitation energy. This has proved to be absolutely necessary for analyzing our correlation data because the theoretical correlation functions are in general very sensitive to the parameters of the γ transitions. It was our purpose to measure p - γ correlation functions of the reaction $^{52}\text{Cr}(d, p\gamma)^{53}\text{Cr}$ as a function of the particle angles for two positions of the γ detector, in and perpendicular to the reaction plane.

One aim was to study whether the DWBA can describe the angular correlation functions in addition to the differential cross section, and whether the correlation experiments yield further information about the reaction mechanism, especially in comparison to differential cross section analyses. In this connection especially, ambiguities in the optical potential are of interest. These ambiguities, which arise in the analyses of the scattering data, can hardly be restricted by analyses of the (d, p) cross sections.

II. THEORY

The theory of particle- γ angular correlations, which has been developed for the axially symmet-

ric case in detail, e.g. by Rose and Brink,⁴ has been extended to the general case by Rybicki, Tamura, and Satchler.⁵ In the following we sum up some details from Ref. 5, important for the present work.

Consider a reaction $A(a, b)B(\gamma)C$. The projectile a and the target nucleus A are unpolarized and the polarization of the emitted particle b and of the γ radiation are not observed. The double differential cross section for coincident measurement of the ejectile b with the polar angles θ_b , ϕ_b and the γ -radiation $B \rightarrow C$ with the angles θ_γ , ϕ_γ is given by

$$\frac{d^2\sigma}{d\Omega_b d\Omega_\gamma} = \frac{1}{4\pi} \frac{\Gamma_{\gamma C}^B}{\Gamma^B} W(\theta_\gamma, \phi_\gamma, \theta_b, \phi_b) \frac{d\sigma}{d\Omega_b}, \quad (1)$$

where

$\Gamma_{\gamma C}^B$ = branching ratio for the γ transition $B(\gamma)C$,

$\frac{d\sigma}{d\Omega_b}$ = differential cross section for the reaction $A(a, b)B$,

W = angular correlation function.

As can be seen from (1), the additional information, which can be deduced from particle- γ angular correlation experiments in comparison to the measurement of the differential cross section is included in the correlation function W . The correlation function can be expressed as follows:

$$W(\theta_\gamma, \phi_\gamma, \theta_b, \phi_b) = \sum_{KQ} \frac{\rho_{KQ}(J_B)}{\rho_{00}(J_B)} R_K(\gamma) \left(\frac{4\pi}{2K+1} \right)^{1/2} Y_K^Q(\theta_\gamma, \phi_\gamma); \quad (2)$$

that is, there is a factorization of W .

The coefficients $R_K(\gamma)$ include the information concerning the γ -transition $B \rightarrow C$; they depend on the spins J_B and J_C and on the multipolarity of the γ radiation. The statistical tensors ρ_{KQ} describe the transition $A(a, b)B$. They can be expressed by means of the density matrix

$$\rho_{KQ}(J_B) = \sum_{M_B, M_B'} \rho_{M_B M_B'} (-)^{J_B - M_B'} (J_B J_B M_B - M_B' | KQ). \quad (3)$$

The elements of the density matrix can be expressed in terms of the reaction amplitudes X_{m_a, M_A, m_b, M_B} describing the transitions between the magnetic substates:

$$\rho_{M_B M_B'} = \sum_{m_a, m_b, M_A} X_{m_a M_A m_b M_B}(\theta_b, \phi_b) X_{m_a M_A m_b M_B'}^*(\theta_b, \phi_b). \quad (4)$$

These amplitudes, which depend on the particle angles θ_b , ϕ_b , include the information about the mechanism of the reaction $A(a, b)B$ and can be

compared to reaction models. Hitherto, a reaction sequence of the type $A(a, b)B(\gamma)C$ has been considered.

If the state B decays by a γ cascade, the γ radiation of the first or of one of the following transitions can be observed. In the second case, for each unobserved transition $J_i \rightarrow J_{i+1}$ an attenuation coefficient $U_K(J_i, J_{i+1})$ joins the $R_K(\gamma)$ coefficient. The $U_K(J_i, J_{i+1})$ coefficients depend on the spins J_i, J_{i+1} and the multipolarity of the γ transition $J_i \rightarrow J_{i+1}$. The case of unobserved intermediate radiation can be of some importance for the analysis of the experiment (see, e.g., Sec. IV B).

The differential cross section $d\sigma/d\Omega_b$ is proportional to the trace of the density matrix $\rho_{M_B M_B'}$. For that reason only absolute squares of transition amplitudes contribute to the differential cross section. By way of contrast, the double differential cross section consists of mixed terms of transition amplitudes of different magnetic substates; i.e., in this case off-diagonal elements of the density matrix are involved, too. From this it can be seen what kind of additional information about the reaction mechanism can be extracted from the correlation function.

One gets different independent combinations of transition amplitudes. The weight of each amplitude depends on the magnitude of the spherical harmonics at the respective position of the γ detector. Therefore, if one measures the double differential cross section for a sufficient number of positions of the γ detector, the individual transition amplitudes can be determined in several cases and compared to theoretical predictions (see, for example, Refs. 6 and 2).

Obviously this type of experiment is a more sensitive test of reaction models than the usual measurements of the differential cross sections. Moreover, interference effects can appear because not only absolute squares but also phase-dependent mixed terms of transition amplitudes contribute to the double differential cross section. Similar effects can also occur at other types of experiments, for example at the measurements of the analyzing power with polarized projectiles.

III. EXPERIMENT

The measurements were performed at the Erlangen tandem van de Graaff accelerator at a deuteron bombarding energy of 10.00 MeV. The double differential cross sections of the reaction $^{52}\text{Cr}(d, p\gamma)^{53}\text{Cr}$ were measured for two positions of the γ detector, placed at 90° in, and perpendicular to, the reaction plane. Thereby the coincident proton groups were detected from 20 to 160° in steps of 10° up to an excitation energy in ^{53}Cr of about 5 MeV. In addition, the differential cross section

was measured from 15 to 165° in steps of 5°. Our data are in good agreement with differential cross section data available at forward angles.^{7,8}

For the spectroscopy of the proton groups a multidetector arrangement consisting of 8–11 silicon surface barrier detectors (with a depletion layer 1800 μm , a resistivity of 32 $\text{k}\Omega\text{cm}$, and a solid angle of 0.5×10^{-3} sr up to 8×10^{-3} sr) was used. The γ radiation was measured by a Ge(Li) detector of 45 cm^3 volume.

For the correlation measurements a self-supporting ^{52}Cr foil (Union Carbide) enriched to 99–99.9%, having a thickness of 0.89 mg/cm^2 , was used. This thickness was chosen to obtain a sufficient energy resolution of the proton spectra and a divergence of the beam after the target small enough to measure the beam current with sufficient accuracy.

Thus each run needed a measuring time of some 40 hours. Two runs were necessary to get the angular correlation in the whole range of the particle angles for one position of the γ detector. The current of the deuteron beam of 10–30 nA, which was stopped in a biased tantalum cup, was measured with an accuracy of about 2% using a current integrating system. The reaction chamber and the γ detector were shielded with lead against background radiation.

The block diagram of the electronics is shown in Fig. 1. The time marking signals of the particle detectors (P1–P11) were derived by use of lead-

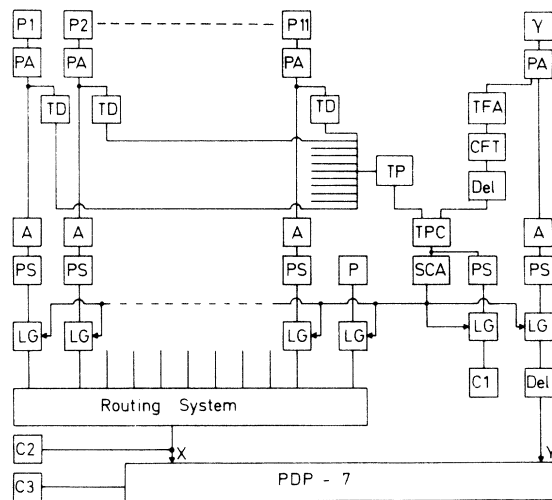


FIG. 1. Block diagram of the electronics: P1–P11, particle detectors; PA, preamplifiers; TD, threshold discriminators; TFA, timing filter amplifier; CFT, constant fraction triggering; Del, delay lines; TPC, time-to-pulse-height converter; SCA, single channel analyzer; A, amplifiers; PS, pulse stretchers; LG, linear gates; P, pulse generator; C1–C3, additional test points.

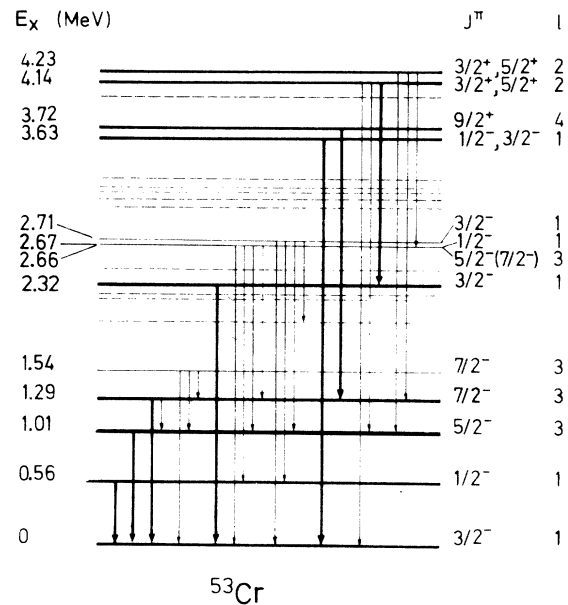


FIG. 2. Decay scheme of ^{53}Cr . The investigated levels and γ transitions are marked by thick solid lines. The levels marked by dashed lines were not observed in the present experiment.

ing-edge triggering with threshold discriminators, whereas the time signals of the γ detector were obtained by use of constant fraction triggering. The p - γ coincidence was determined with a time-to-pulse-height converter followed by a single channel analyzer. To process high counting rates the stretched energy signals of each particle branch were fed into a gate before entering the routing system. The experiment was controlled on line by additional test points (C1–C3). The rest of the electronics has been described elsewhere.³

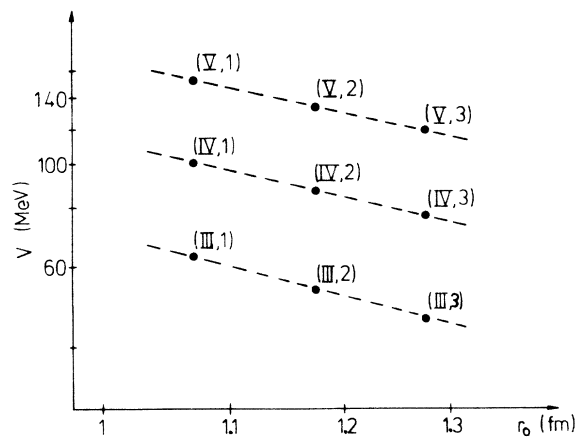


FIG. 3. (V_0, r_0) ambiguities. The Roman numerals correspond to the number of half wave lengths, the Arabic numerals, to values of r_0 .

The acquisition and evaluation of the data were carried out two dimensionally (4096×1024 channels).

The evaluation of the double differential cross sections was performed by projecting the data matrix and integrating the photopeak in the γ spectra as described in Ref. 3. The photopeak efficiency and the solid angle of the γ detector were determined as a product in the energy range of 0.511 to 4.43 MeV by use of standard sources. In favorable cases (large cross section, low γ energy, branching ratio near 100%) the errors were about 3%. The uncertainty at the peak integration and the current measurement were also taken into account.

The influence of random coincidences was studied in detail in Ref. 9. For the present case it turned out that random coincidences give negligible errors.

IV. RESULTS AND DISCUSSION

In the present work the differential and double differential cross sections of several strong transitions with $l=1, 3,$ and 4 of the reactions $^{52}\text{Cr}(d, p)^{53}\text{Cr}$ and $^{52}\text{Cr}(d, p\gamma)^{53}\text{Cr}$ were measured absolutely. From these quantities the associated experimental angular correlation functions have been obtained. The differential cross sections and the angular correlation functions were analyzed by zero

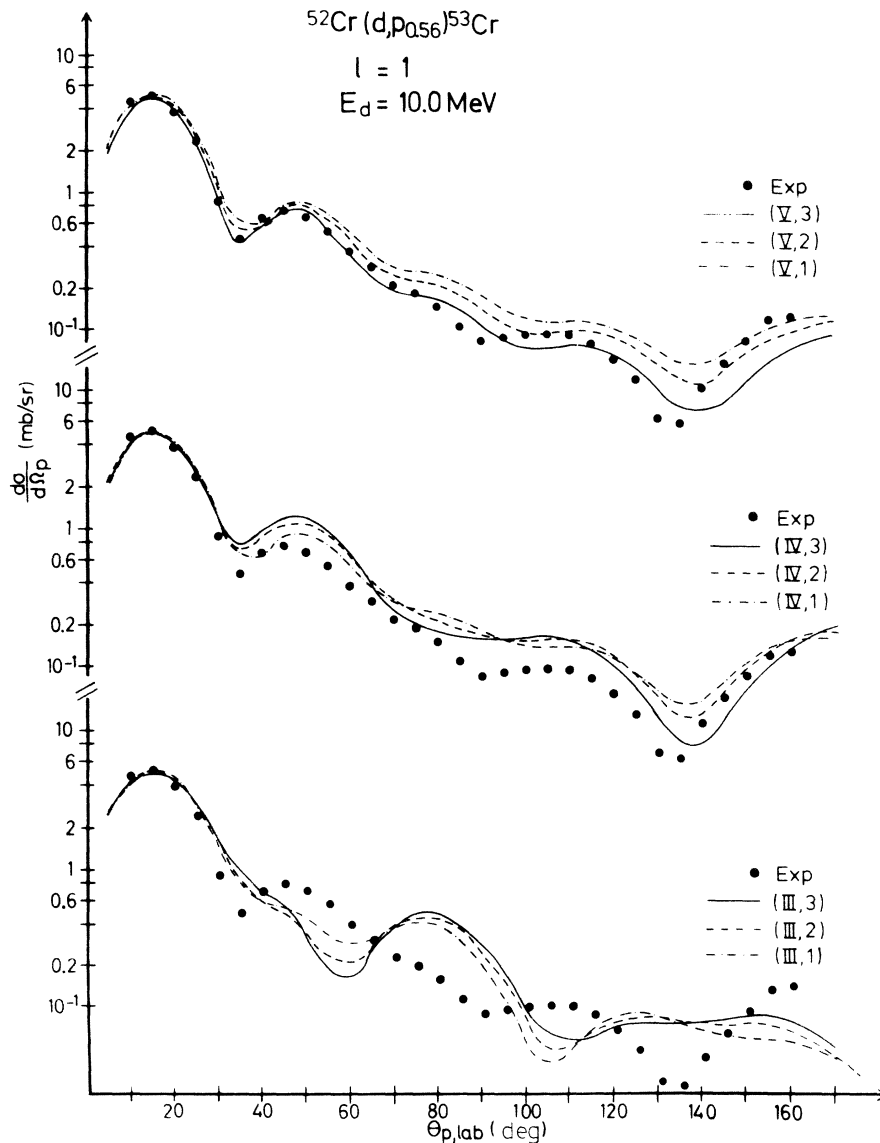


FIG. 4. Experimental differential cross section of the reaction $^{52}\text{Cr}(d, p_{0.56})^{53}\text{Cr}$ and DWBA analyses.

range DWBA. In Fig. 2 the decay scheme^{10, 11} of ⁵³Cr is shown in the range of excitation energy considered in the present work. The branching and mixing ratios needed for the calculation of the angular correlation functions are also taken from Refs. 10 and 11.

The calculations of the differential cross sections and the angular functions were performed by means of the DWBA code VENUS.^{12, 13} The differential cross sections have been calculated in addition by means of the code DWUCK.¹⁴ In order to calculate the distorted waves of the deuterons and protons usual optical potentials $U(r) = V(r) + iW(r)$

+ $V_c(r)[+V_{so}(r)]$ of Woods-Saxon type with surface absorption were used; $V_c(r)$ is the usual Coulomb potential. The calculations have been done with and without a Thomas spin orbit potential, respectively. The form factor was calculated by means of a real Woods-Saxon potential, also with or without a spin orbit term.

In analyzing the scattering data of many nuclei and projectiles so-called "potential families" have been found in the real part of the optical potential, i.e. for a fixed value of the radius parameter r_0 there exist several discrete values for the depth V_0 which fit the data equivalently. These potential

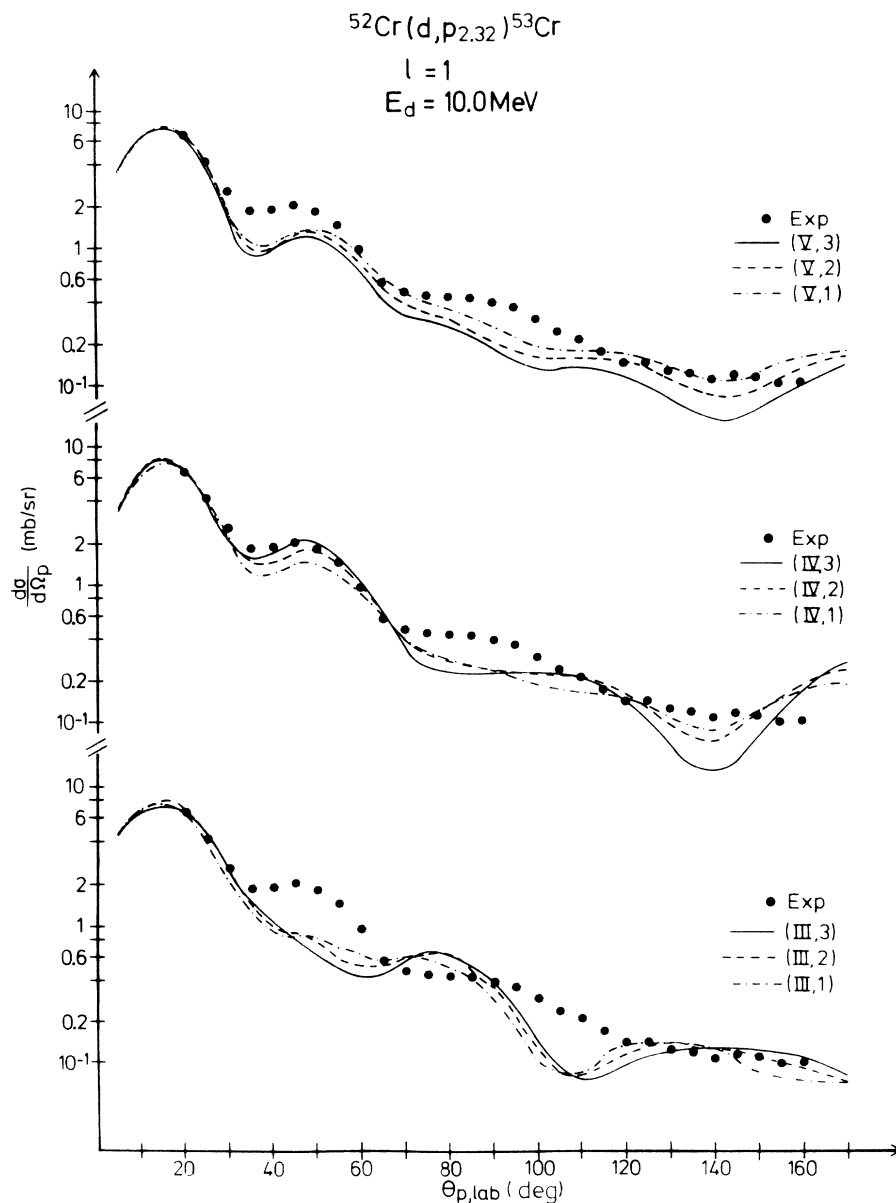


FIG. 5. Experimental differential cross section of the reaction $^{52}\text{Cr}(d, p_{2,32})^{53}\text{Cr}$ and DWBA analyses.

families are distinguished by the number of half wave lengths of the wave functions inside of the potential well. Each of these families is associated with a certain depth of the imaginary potential. Besides this discrete ambiguity a continuous ambiguity of the form $V_0 r_0^k = \text{const}$ (with $1 \leq k \leq 2$) exists at each family. Such ambiguities have been investigated in more detail in Ref. 15.

The elastic scattering of deuterons of 10 MeV bombarding energy from ^{52}Cr has been analyzed by Andrews *et al.*,¹⁶ who also found these potential ambiguities. In the present work the potentials

given in Ref. 16 have been transformed into Woods-Saxon form and modified in order to describe the differential cross section of the (d, p) reaction as well as possible and still get a good agreement with the scattering data.

For a systematic analysis three families (giving 3, 4, and 5 half wave lengths) were taken at three different values for the radius parameter. The doubles used, (V_0, r_0) , are shown in Fig. 3. For the calculations of the distorted waves of the protons emitted in the (d, p) reaction the "best fit" parameters of Ref. 17 were used.¹⁸

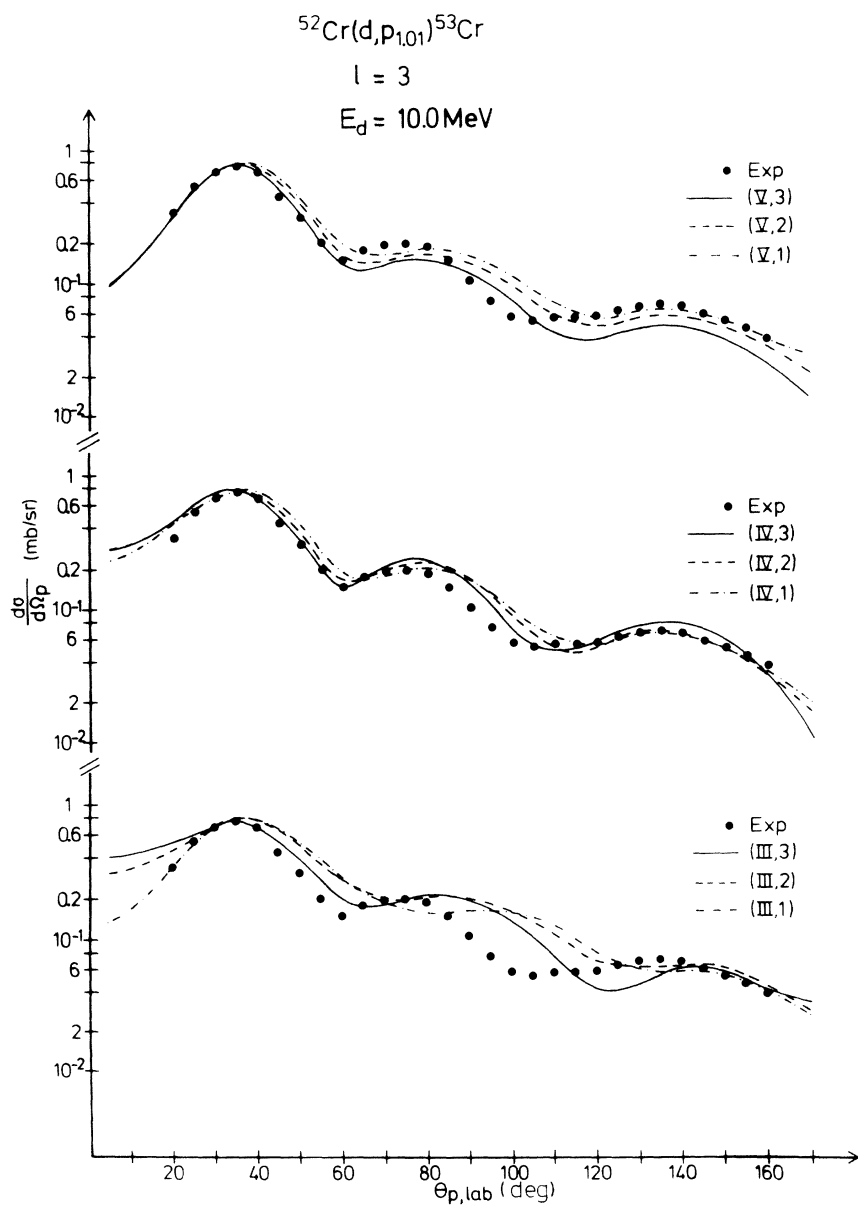


FIG. 6. Experimental differential cross section of the reaction $^{52}\text{Cr}(d, p_{1,01})^{53}\text{Cr}$ and DWBA analyses.

A. Analyses of the differential cross sections

In Figs. 4-7 the angular distributions of the absolute differential cross section are shown for several (d, p) transitions belonging to $l=1, 3,$ and 4 in comparison with DWBA calculations. The calculations have been carried out with deuteron potentials giving three half wave lengths (lower part of each figure), four half wave lengths (middle part), and five half wave lengths (upper part), respectively. The solid, dashed, and dashed-dotted lines belong to the different (V_0, r_0) doubles within one $(V_0 r_0^2)$ family of the deuteron potential, respectively. For the calculation of the form factor

values of $r_0 = 1.3$ fm and $a_0 = 0.7$ fm were used. The influence of the spin orbit potential on the shape of the angular distribution turned out to be very small; hereby, slight variations of the spectroscopic factors could be observed.

On the whole the investigations of the differential cross section have shown that DWBA calculations using deuteron potentials giving four and five half wave lengths can well reproduce the discussed transitions with $l=1, 3,$ and 4 for θ_p between 20 and 160° . For potentials giving three half wave lengths the agreement for the $l=1$ transitions is insufficient. For the $l=3$ transition the fits become somewhat better. For the $l=4$ transition the

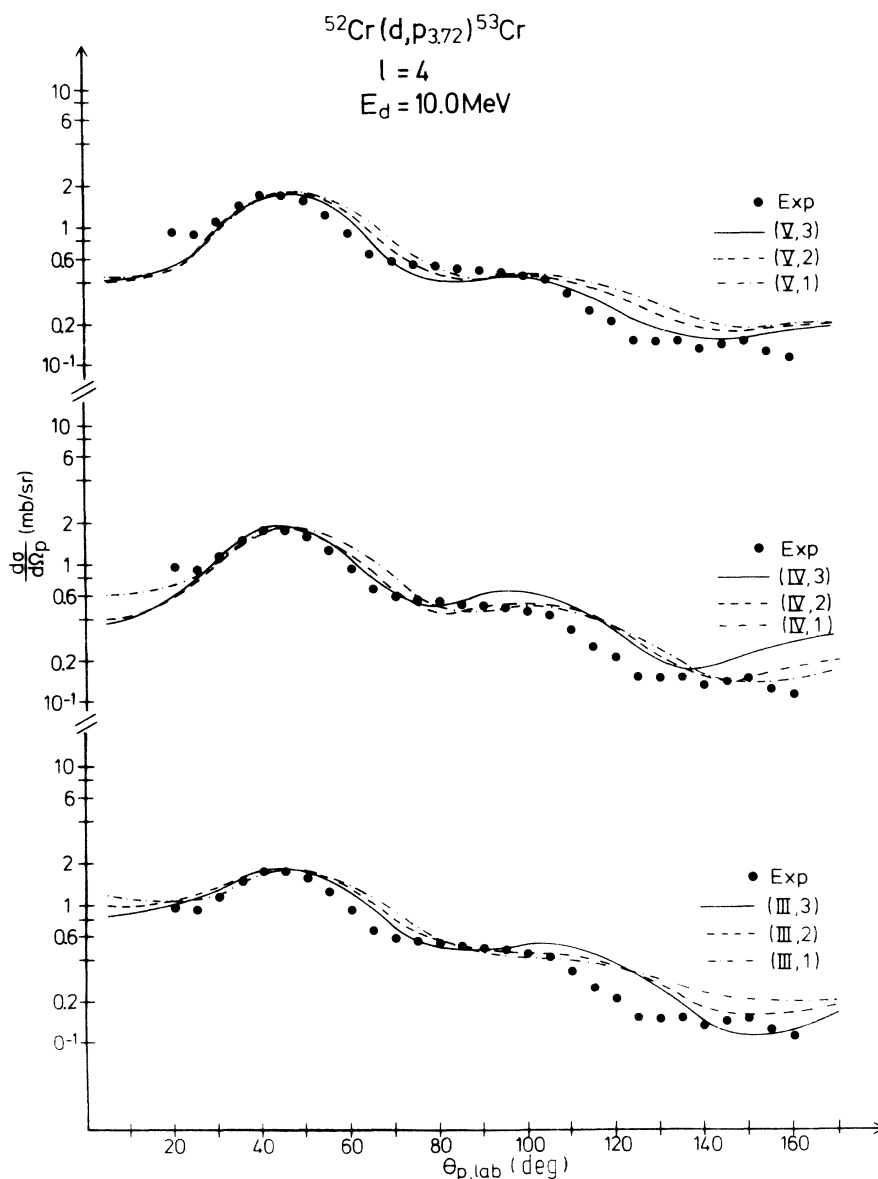


FIG. 7. Experimental differential cross section of the reaction $^{52}\text{Cr}(d, p_{3,72})^{53}\text{Cr}$ and DWBA analyses.

agreement for the different half wave lengths are equivalent. Similar statements are given in Ref. 19.

The present investigation shows that the differential cross sections belonging to $l=1$ transitions respond more sensitively to the potential parameters than, say, the transitions with $l=4$. This can be understood from the structure of the differential section. In the case of $l=4$ a large number of transition amplitudes contribute to the differential cross section. As these transition amplitudes are added incoherently, it is possible that differences between the corresponding transition amplitudes, which arise from using different potential parameters, can be compensated in the differential cross section. In the case of $l=1$ transitions the number of summands is smaller so that the differences between the transition amplitudes still remain visible.

B. Analyses of the angular correlation functions

The correlation functions for the $l=1$ transition to the first excited level in ^{53}Cr ($E_x=0.56$ MeV, $J_B^\pi = \frac{1}{2}^-$) with subsequent deexcitation to the ground state are shown in Fig. 8 for both positions of the γ detector. In the case of $J_B = \frac{1}{2}$ the theoretical angular correlation function $W=1$ is independent of the reaction mechanism. Obviously our experimental values agree with the theoretical predictions of $W=1$. Therefore we can exclude systematic errors.

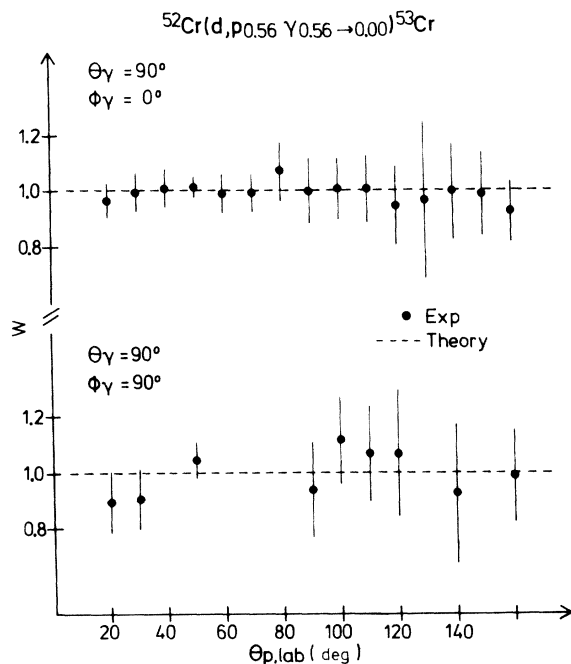


FIG. 8. Experimental and theoretical angular correlation functions for the reaction $^{52}\text{Cr}(d, p_{0.56}\gamma_{0.56 \rightarrow 0.00})^{53}\text{Cr}$.

Discrete ambiguities of the optical potential

As shown, the differential cross section of the $l=1$ transition leading to the level with $E_x=2.32$ MeV is well described by the potentials used, giving four and five half wave lengths. This level decays entirely to the ground state. In Fig. 9 the experimental angular correlation functions are compared to DWBA calculations. Deuteron potentials giving three, four, and five half wave lengths with radius parameter $r_0=1.275$ fm have been taken for the analysis. If no spin orbit term is used, for correlation functions describing $l=1$ transitions to $J_B = \frac{3}{2}$ the theory yields, for the position of the γ detector perpendicular to the reaction plane, $W = \text{const}$, independent of the potential parameters. Our experimental data are in good agreement with this theoretical value (lower part in Fig. 9). For these reasons the discussion of the various potential families is done by the in-plane correlation functions (upper part of Fig. 9). The deuteron potentials giving three and five half wave lengths obviously yield an agreement with the experimental data being not as good as that yielded by the potential giving four half wave lengths (especially in the region of the experimental minimum at $\theta_p=40^\circ$).

The angular correlation functions for the $l=3$ transition to the $\frac{5}{2}^-$ state at $E_x=1.29$ MeV decaying 100% to the ground state was also analyzed. Though

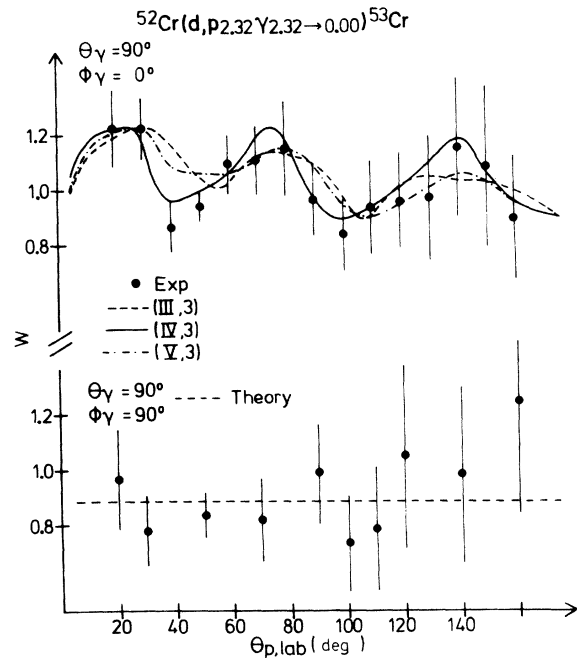


FIG. 9. Experimental angular correlation functions for the reaction $^{52}\text{Cr}(d, p_{2.32}\gamma_{2.32 \rightarrow 0.00})^{53}\text{Cr}$ and DWBA analyses with optical potentials giving different half wave lengths.

the correlation functions are affected by rather high statistical errors it can also be concluded that for this transition the deuteron potential giving four half wave lengths yields the best agreement with the experimental data.

The $\frac{9}{2}^+$ state at $E_x = 3.72$ MeV, which is strongly populated by an $l=4$ transition, decays 100% to the $\frac{5}{2}^-$ state at $E_x = 1.29$ MeV. Both this γ transition and the subsequent γ transition to the ground state were studied. In Fig. 10 the experimental and theoretical correlation functions of the transition 1.29 MeV \rightarrow 0.00 MeV are shown as an example of a correlation with unobserved intermediate radiation. It can also be seen that for this transition our experimental correlation data are described well by DWBA. The best agreement is found again by using potentials giving four half wave lengths (compare the various fits for particle angles $100^\circ \leq \theta_p \leq 120^\circ$ for both positions of the γ detector).

For the reaction $^{52}\text{Cr}(d, p\gamma)^{53}\text{Cr}$ it is possible to describe the angular correlation data for the strong transitions well by DWBA. Moreover, it is shown that discrete ambiguities in the optical potentials can be restricted by means of the correlation function more than by means of the differential cross section.

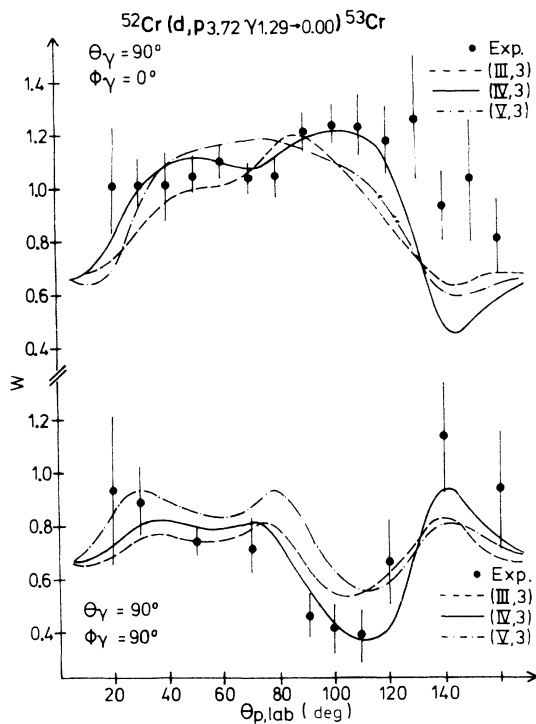


FIG. 10. Experimental angular correlation functions for the reaction $^{52}\text{Cr}(d, p_{3.72}\gamma_{1.29 \rightarrow 0.00})^{53}\text{Cr}$ and DWBA analyses with optical potentials giving different half wave lengths.

Continuous ambiguities of the optical potential

It was possible to study the discrete ambiguities of the optical potential without respect to the continuous ambiguities $V_0 r_0^k = \text{const}$, because it turned out that these produce very small variations in the correlation functions. This is exemplified in Fig. 11 for the $l=1$ transition to the level at $E_x = 2.32$ MeV with deuteron potentials giving five half wave lengths.

It turned out that for the reaction $^{52}\text{Cr}(d, p\gamma)^{53}\text{Cr}$ the continuous ambiguities within the different potential families cannot be restricted by means of the correlation functions for any l value, studied here.

The parameters of the neutron potentials

A variation of the parameters of the neutron potential makes itself felt mainly in the value of the spectroscopic factor, as shown in detail, for instance, in Ref. 20. The shape of the angular distribution of the differential cross section is scarcely affected. In extracting the angular correlation function from the differential and double differential cross section one eliminates the spectroscopic factor. Therefore, by a variation of the parameters of the neutron potential in reasonable limits, the angular correlation function is changed negligibly and gives no further information about the spectroscopic factor.

Spin orbit potentials

The angular distributions of the differential cross sections calculated by DWBA are influenced little by addition of spin-orbit potentials. In the angular correlation functions mixed terms of transition amplitudes are also involved. Therefore, the question arises whether spin orbit terms may affect the correlation function in a more sensitive way than the differential cross section. The calculations show

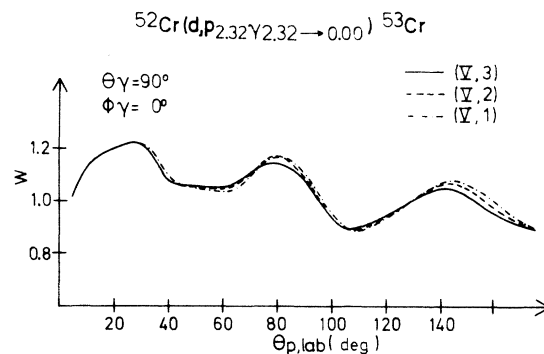


FIG. 11. DWBA angular correlation functions with optical potentials giving five half wave lengths.

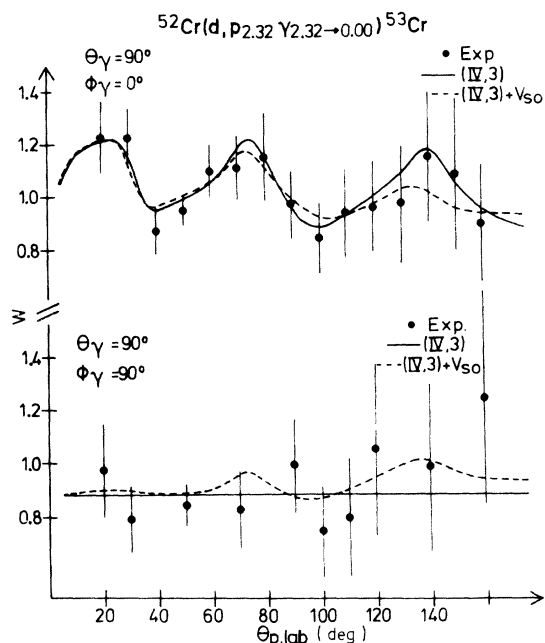


FIG. 12. Experimental angular correlation functions for the reaction $^{52}\text{Cr}(d, p_{2.32}\gamma_{2.32 \rightarrow 0.00})^{53}\text{Cr}$ and DWBA analyses with and without spin-orbit potentials.

that by addition of spin-orbit potentials the shape of the angular correlation function is smeared out and the phases are somewhat shifted. Figure 12 (upper part) exemplifies this result for the transition

$$^{52}\text{Cr}(d, p_{2.32}\gamma_{2.32 \rightarrow 0.00})^{53}\text{Cr}.$$

The theoretical fits were calculated using the potential (IV, 3) with and without spin orbit term,²¹ respectively. The effect of spin orbit potentials for $l=1$ transitions can be seen from Fig. 12 (lower part). In this case the theory gives structures in the angular correlation function for the position of the γ detector perpendicular to the reaction plane. As the variations among different theoretical fits are small, no spin orbit potential is re-

quired to describe the experimental data. Similar results have been found for the transitions

$$^{52}\text{Cr}(d, p_{1.01}\gamma_{1.01 \rightarrow 0.00})^{53}\text{Cr},$$

$$^{52}\text{Cr}(d, p_{3.72}\gamma_{3.72 \rightarrow 1.29})^{53}\text{Cr},$$

and

$$^{52}\text{Cr}(d, p_{3.72}\gamma_{1.29 \rightarrow 0.00})^{53}\text{Cr}.$$

The reaction $^{52}\text{Cr}(d, p)^{53}\text{Cr}$ was also investigated with vector-polarized and tensor-polarized deuterons by Haerberli *et al.*^{22, 23} One of their deuteron potentials, which also gives four half wave lengths, has been included in our analyses. The shape of the experimental correlation functions could also be described by this potential in a satisfactory way.

The main purpose of this work has been to show by means of the reaction $^{52}\text{Cr}(d, p\gamma)^{53}\text{Cr}$, how much new information about the reaction mechanism can be obtained by particle- γ correlation experiments. It would be desirable to analyze not only the correlation function but also the individual transition amplitudes in order to find out if special models are suitable to describe the reaction mechanism. As in most reactions the determination of individual transition amplitudes is very difficult, one looks for quantities which are functions of the transition amplitudes and which can be measured in a relatively simple way. A very simple quantity of this type is the differential cross section. If the differential cross section is well described by any reaction theory, it may be expected that the individual transition amplitudes are described by this theory, too.²⁴ In order to examine whether this expectation proves true, it is necessary to study other and independent quantities which are also sensitive to the transition amplitudes, as for instance double differential cross sections, analyzing powers, or γ ray circular polarization.

As shown in the present work, there are potentials which can describe both the differential cross section and the angular correlation function; and there are other potentials which can describe only the differential cross section.

¹A. E. Litherland and A. J. Ferguson, *Can. J. Phys.* **39**, 788 (1961).

²H. Wagner, A. Hofmann, and F. Vogler, *Phys. Lett.* **47B**, 497 (1973).

³F. Vogler, M. Berg, A. Hofmann, and H. Wagner, *Phys. Rev. C* **9**, 242 (1974).

⁴H. J. Rose and D. M. Brink, *Rev. Mod. Phys.* **39**, 306 (1967).

⁵F. Rybicki, T. Tamura, and G. R. Satchler, *Nucl. Phys.* **A146**, 659 (1970).

⁶T. D. Hayward and F. H. Schmidt, *Phys. Rev. C* **1**,

923 (1970).

⁷R. Bock, H. H. Duhm, S. Martin, R. Rüdél, and R. Stock, *Nucl. Phys.* **72**, 273 (1965).

⁸J. L. Alty, L. L. Green, G. D. Jones, and J. F. Sharpey-Schafer, *Nucl. Phys.* **86**, 65 (1966).

⁹To be published.

¹⁰T. P. G. Carola, W. C. Ohlsen, D. M. Sheppard, B. D. Sowerby, and P. J. Twin, *Nucl. Phys.* **A144**, 53 (1970).

¹¹T. P. G. Carola and J. G. Tamboer, *Nucl. Phys.* **A185**, 81 (1972).

¹²T. Tamura, W. R. Coker, and F. Rybicki, *Comput.*

Phys. Commun. 2, 94 (1971).

- ¹³In a first step the program calculates the individual transition amplitudes $X_{m_a M_A m_b M_B}$. Usually, as in our case, these transition amplitudes are not available from the experiment because of the variety of involved magnetic substates. Therefore, in a second step the transition amplitudes are combined to give the quantities available by the experiment, e.g., the differential cross section and the angular correlation function.
- ¹⁴P. D. Kunz, University of Colorado Reports Nos. C00535-613 and 535-606.
- ¹⁵M. E. Cage, A. J. Cole, and G. J. Pyle, Nucl. Phys. A201, 418 (1973).
- ¹⁶P. T. Andrews, R. W. Clift, L. L. Green, J. F. Sharpey-Schafer, and R. N. Maddison, Nucl. Phys. 56, 422 (1964).
- ¹⁷F. D. Becchetti and G. W. Greenlees, Phys. Rev. 182, 1190 (1969).
- ¹⁸Although potential ambiguities have mostly been found for the scattering of d , ^3He , and α , ambiguities can also occur for the scattering of protons. In the present work only ambiguities of the deuteron potential have been investigated.
- ¹⁹J. L. Alty, L. L. Green, G. D. Jones, and J. F. Sharpey-Schafer, Nucl. Phys. 86, 65 (1966).
- ²⁰U. Scheib, A. Hofmann, G. Philipp, and F. Vogler, Nucl. Phys. A203, 177 (1973).
- ²¹Spin orbit potentials were added in the entrance as well as in the exit channel, because analysis after addition of a spin orbit term in only one channel yielded even smaller variation between the different fits.
- ²²N. Rohrig and W. Haeberli, Nucl. Phys. A206, 225 (1973).
- ²³D. S. Kocher and W. Haeberli, Nucl. Phys. A196, 225 (1972).
- ²⁴It has been shown, however, that this is not always valid; compare Ref. 2.